

P. Ramoino · P. Fronte · M. Fato · F. Beltrame  
M. Robello · A. Diaspro

## Fluid phase and receptor-mediated endocytosis in *Paramecium primaurelia* by fluorescence confocal laser scanning microscopy

Received: 12 October 2000 / Revised version: 24 April 2001 / Accepted: 10 May 2001 / Published online: 3 July 2001  
© EBSA 2001

**Abstract** In ciliated protozoa, most nutrients are internalized via phagocytosis by food vacuole formation at the posterior end of the buccal cavity. The uptake of small-sized molecules and external fluid through the plasma membrane is a localized process. That is because most of the cell surface is internally covered by an alveolar system and a fibrous epiplasm, so that only defined areas of the cell surface are potential substance uptake sites. The purpose of this study is to analyze, by fluorescence confocal laser scanning microscopy, the relationship between WGA (*Triticum vulgaris* agglutinin) and dextran internalization in *Paramecium primaurelia* cells blocked in the phagocytic process, so that markers could not be internalized via food vacuole formation. WGA, which binds to surface constituents of fixed and living cells, was used as a marker for membrane transport and dextran as a marker for fluid phase endocytosis. After 3 min incubation, WGA-FITC is found on plasma membrane and cilia, and successively within small cytoplasmic vesicles. After a 10–15 min chase in unlabeled medium, the marked vesicles decrease in number, increase in size and fuse with food vacuoles. This fusion was evidenced by labeling food vacuoles with BSA-Texas red. Dextran enters the cell via endocytic vesicles which first localize in the cortical region, under the plasma membrane, and then migrate in the cytoplasm and fuse with other endocytic vesicles and food vacuoles. When cells are fed with WGA-FITC and

dextran-Texas red at the same time, two differently labeled vesicle populations are found. Cytosol acidification and incubation in sucrose medium or in chlorpromazine showed that WGA is internalized via clathrin vesicles, whereas fluid phase endocytosis is a clathrin-independent process.

**Keywords** WGA · Dextran · Clathrin inhibitors · Fluorescence CLSM · Ciliated protozoa

### Introduction

Fluid phase and receptor-mediated endocytosis has been extensively studied in mammalian cells (Mellman et al. 1987; Courtoy 1989; Gruenberg and Howell 1989; van Deurs et al. 1989) and most of what is understood about the endocytic process in protozoa comes from studies of pinocytosis in amoebae (Chapman-Andresen 1962; Stockem and Wohlfarth-Bottermann 1969; Stockem 1977). The limited data about receptor-mediated endocytosis in ciliates is also due to the difficulty of visualizing this process at an optical level. Indeed, in ciliates, only defined areas on the cell surface are potential sites for endocytic uptake since most of the surface is covered internally by an extensive system of alveoli and an underlying fibrous epiplasm (Allen 1988). This system is interrupted only at the cytopharynx, the cytoproct, contractile vacuole pores and along the junctions of the abutting units of alveolar membrane sacs. Only the punctuate indentations of the plasma membrane, called parasomal sacs, and pellicular pores are potential endocytic entry ports of all fluid phase and putative receptor-mediated endocytosis (Nilsson and van Deurs 1983; Allen et al. 1992; Allen and Fok 1993).

Detailed morphological and tracer studies on endocytosis carried out by electron microscopy showed that, in *Paramecium multimicronucleatum*, fluid phase markers such as horseradish peroxidase (HRP), and, in *Tetrahymena pyriformis*, receptor-mediated markers such as cationized ferritin, are internalized via coated

P. Ramoino (✉) · P. Fronte  
DIP.TE.RIS., University of Genoa,  
Corso Europa 26, 16132 Genoa, Italy  
E-mail: ramoino@diptesis.unige.it  
Tel.: +39-010-3538030  
Fax: +39-010-3538209

A. Diaspro · M. Robello  
INFM and Department of Physics, University of Genoa,  
Via Dodecaneso 33, 16146 Genoa, Italy

M. Fato · F. Beltrame  
Department of Communication,  
Computer and System Sciences (DIST),  
University of Genoa, Viale Causa 13, 16145 Genoa, Italy

pits and are found in coated vesicles (Nilsson and van Deurs 1983; Allen et al. 1992). Both coated pits and vesicles are also labeled in fixed cells when a monoclonal antibody against the plasma membrane of *P. multimicronucleatum* (C6 antigen) is applied to cryosections, suggesting that both membrane-bound and fluid phase markers are internalized at the coated pits (Allen et al. 1992). Most endocytotic sites are clathrin-coated pits; however, there is increasing evidence in mammalian cells for clathrin-independent pathways, mediated by caveolae or non-coated vesicles (Lamaze and Schmid 1995).

The scope of this work is to study the relationship between WGA (*Triticum vulgaris* agglutinin) and dextran internalization in *P. primaurelia* cells blocked in the phagocytic process, so that markers could not be internalized via food vacuole formation. WGA, which binds to surface constituents of fixed (Allen et al. 1988; Ramoino 1997) and living cells, was used as a marker for membrane transport and dextran as a marker for fluid phase endocytosis.

## Materials and methods

### Chemicals

10,000 dextran-Texas red (TXR) was obtained from Molecular Probes (Eugene, Ore., USA). *Triticum vulgaris* agglutinin conjugated with fluorescein isothiocyanate (WGA-FITC), bovine serum albumin conjugated with Texas red (BSA-TXR) or with fluorescein isothiocyanate (BSA-FITC), chlorpromazine, filipin, nystatin and the other chemicals were purchased from Sigma (Germany).

### Cell cultivation

*Paramecium primaurelia* stock 90 was grown at 25 °C in lettuce medium (pH 6.9) bacterized with *Enterobacter aerogenes*. Cells were harvested in the mid-log phase of growth.

### Blocking of phagocytic activity

Cells were pre-treated for 15 min with trifluoperazine, a calmodulin antagonist that has been shown to inhibit *Paramecium* phagocytosis (Allen et al. 1992). The effective dose (2.5–5 µg/mL) required to block the uptake of latex particles was estimated prior to each experiment.

### Marker uptake and intracellular flow

Living cells were pulsed continuously in sterile medium containing either WGA-FITC (50 µg/mL) or dextran-TXR (0.2 mg/mL) for times of 30 s as well as 1, 2, 3 and 5 min before fixation. Additional cells were pulsed for 3 min and chased in fresh unlabeled medium for 5, 10, 15, 20, 30, 45 and 60 min. Cells were fixed at room temperature for 30 min in 2% paraformaldehyde in 0.1 M phosphate buffer (pH 7.4).

### Double labeling experiments

In additional experiments, in order to analyze the relationship between the endocytic vesicles and the phagosome-lysosome system vesicles, cells were first fed for 30 min with BSA-TXR or BSA-FITC (0.2 mg/mL final concentration) and latex particles (0.3 µm

diameter, 0.2 mg/mL), washed and then processed as described above (inhibition of phagocytosis and labeling with WGA-FITC or with dextran-TXR).

The relationship between the markers internalized via fluid phase and membrane-mediated transport was studied by pulsing continuously the cells both with 50 µg/mL WGA-FITC and 0.2 mg/mL dextran-TXR for 30 s as well as 1, 2, 3, 5 and 10 min, or by pulsing the cells for 5 min and fixing them after a 0, 5, 10, 15, 20, 30, 40, 50 and 60 min chase in unlabeled medium.

### Inhibitory treatments

To study the effect of medium hypertonicity (0.20 M sucrose), cytosol acidification (10 mM acetic acid, pH 5.0), chlorpromazine (0.5 µg/mL), nystatin (2 µg/mL) and filipin (0.1 µg/mL) cells were pulsed continuously in sterile medium containing WGA-FITC (50 µg/mL), dextran-TXR (0.2 mg/mL) and the inhibitors for 2, 5, 10 and 15 min before fixation, with or without pre-incubation in the inhibitors for 15 min. In additional experiments, cells pulsed for 5 min in a medium containing the fluorochromes were washed and fixed after a 5, 10, 20 and 30 min chase in fluorochrome-free medium. The inhibitors were present from the beginning of the pulse to the end of the chase.

### Image acquisition and analysis

Images were acquired by CLSM using a Nikon PCM 2000 (Nikon Instruments, Florence, Italy), an ultracompact laser scanning microscope system based on a galvanometer point-scanning mechanism, a single pinhole optical path and an all-fiber optical system for delivering light, both in excitation and in collection (Diaspro et al. 1999). Volumetric scanning, along the x, y, z axes, was produced at high spatial resolution. Dual channel acquisition, plus a third channel switchable to transmission or to a third fluorescence imaging modality, was performed at a rate of one full 1024×1024 frame every 2 s, assuring a line scan at 2 ms. Integration time ranged from 1.5 to 100 µs. The PCM 2000 scanning head was mounted on an inverted optical microscope (Nikon Eclipse TE 300). An argon-ion laser (488 nm, 514 nm) and a He-Ne laser (543.5 nm), enclosed in a common multi-laser module, provided the excitation beams that were delivered to the scanning head through a single-mode optical fiber plugged directly into the optical scanning head. Photomultiplier tubes (PMTs) were placed within the control unit and the collected light was conveyed through high-transmission optical fibers. This greatly reduced the electronic noise at the PMTs output and saved space inside the scanning head. The microscope was set to standard conditions for fluorescein fluorescence (excitation, 488 nm; emission, 515/530 nm), TRITC fluorescence (excitation, 543.5 nm; emission, 590 nm) and Texas red fluorescence (excitation, 543.5 nm; emission, 620 nm), laser power 1.5 mW with illumination attenuated using a 3% transmission neutral density filter to reduce photobleaching, a 50 µm pinhole diameter and an oil immersion objective 100×/Na = 1.3 (Diaspro et al. 1996).

The software EZ2000 (Coord, Amsterdam, Netherlands) was used for image acquisition, storage and visualization.

Control and inhibitory experiments were repeated 3–4 times and photomicrographs are representative of observations of 30 cells on average in each sample.

## Results

WGA-FITC are internalized via food vacuoles formed at the cytopharynx when it is added to the cell incubation medium without phagocytosis inhibition. Cells pulsed for 3 min (Fig. 1a) show some food vacuoles at the posterior pole of the body. After a 10-min chase in unlabeled medium the number of fluorescent food

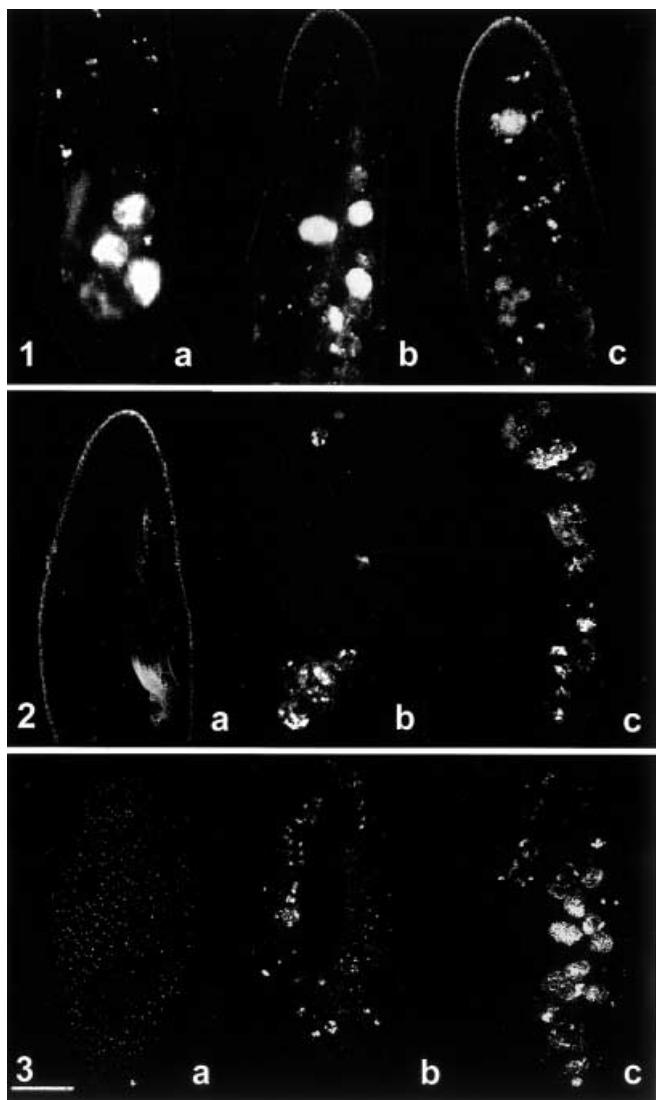


**Fig. 1a–c** Cells fed WGA-FITC for 3 min. Fluorescent lectin is localized within food vacuoles in the posterior end of the cell (**a**). After a 10-min chase in unlabeled medium (**b**) the number of food vacuoles increases as the vacuolar content is digested by lysosomal enzymes and the breakdown substances pass into the cytoplasm through the vacuolar membrane or by way of small pinocytotic vesicles which fuse with other food vacuoles. After a 20-min chase in unlabeled medium the vesicles of the phago-lysosomal system are labeled and after 45 min (**c**) fluorescence is also found on the plasma membrane

**Fig. 2a–c** Cells blocked in phagocytic activity and labeled with WGA-FITC for 3 min. Plasma membrane and small vesicles inside the cell fluoresce (**a**). After a 10-min chase in unlabeled medium (**b**), fluorescence is visible only in a few food vacuoles, whereas after 30 min (**c**) the labeled food vacuole number increases and small vesicles throughout the cytoplasm fluoresce

**Fig. 3a–c** In cells blocked in phagocytic activity and labeled with dextran-TXR for 3 min, fluorescence is visible in small vesicles located in the cortex under the plasma membrane (**a**). After a 10-min chase in unlabeled medium (**b**), vesicles decrease in number and increase in size. After 30 min, several food vacuoles are labeled (**c**) and then the number of vacuoles decreases as vacuolar content is digested and vacuoles are egested at the cytoproct. Bar: 20 µm

vacuoles increases (Fig. 1b). The increase in labeled food vacuoles in a fluorochrome-free medium is due to the fact that the ingested lectins are degraded and pass into the cytoplasm by small vesicles which then fuse with other food vacuoles (Ramoino et al. 1996). Increasing the chase in unlabeled medium increases the fluorescence inside the cytoplasm, which is found later in the vesicles of the phagosome-lysosome system and at the plasma membrane level (Fig. 1c). Conversely, when phagocytosis is blocked by trifluoperazine, the fluorescence is initially found, in 3 min pulsed cells, on the plasma membrane and cilia and inside the cell in small cytoplasmic vesicles (Fig. 2a). After a 5–10 min chase in unlabeled medium, fluorescent vesicles fuse with some food vacuoles (Fig. 2b), and after 20–30 min the labeled food vacuoles increase in number (Fig. 2c). Therefore, the digestion inside the vacuoles of lectins internalized via endocytosis begins later with respect to lectins internalized via food vacuole formation (phagocytosis). Moreover, a very weak fluorescence is detectable on a plasma membrane after longer time periods compared with lectin internalization via food vacuole formation.

The fusion of endocytic vesicles with food vacuoles is evidenced by a double-labeling experiment in which the vesicles are dyed with WGA-FITC and the food vacuoles with BSA-TXR (data not shown).

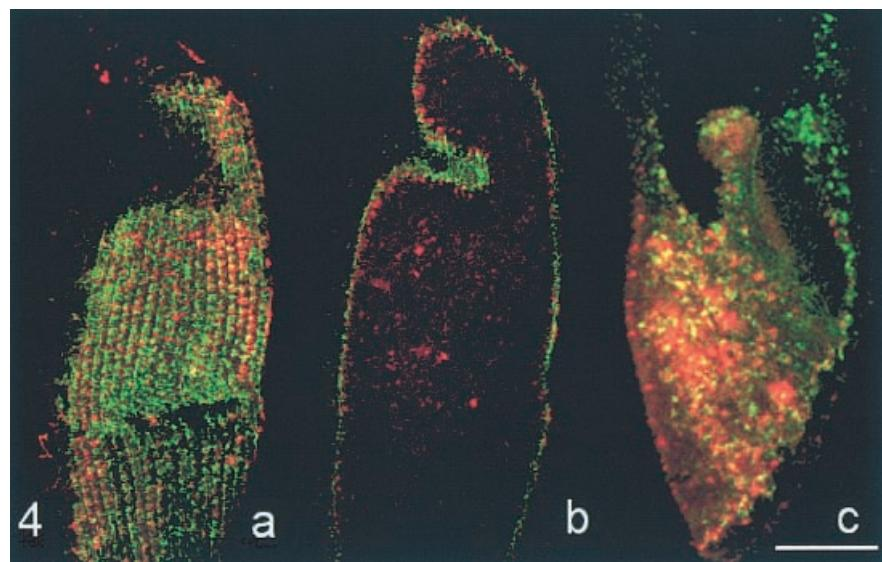
Dextran-TXR (fluid phase endocytosis marker) does not label the plasma membrane and enters the cell via small vesicles initially localized at the cortical level (Fig. 3a). The vesicles later migrate in the cytoplasm and fuse with other endocytic vesicles and with food vacuoles (Fig. 3b). The number of labeled food vacuoles increases as the dextran-labeled vesicles fuse with food vacuoles (Fig. 3c) and then decreases when the vacuolar content is digested and food vacuoles containing the indigestible material are ejected at the cytoproct.

The relationships between the two different routes of internalization, membrane transport and fluid phase endocytosis, are clearly shown when cells blocked in their phagocytic activity are simultaneously fed with WGA-FITC and dextran-TXR (Fig. 4). The data obtained by confocal microscopy suggest that WGA and dextran are present in different endocytic vesicles soon after initiation of uptake (< 10 min). The two probes probably partly join prior to their fusion with the phago-lysosomal compartment.

From these data we can assume that dextran-TXR and WGA-FITC enter the cells through two different vesicle populations. Since studies carried out on mammalian cells showed that incubation in a sucrose medium (Daukas and Zigmond 1985) and cytosol acidification by acetic acid (Davoust et al. 1987; Sandvig et al. 1987) inhibit clathrin-mediated endocytosis, we tested the effect of such inhibitors on WGA and dextran endocytosis.

After 5, 10 and 15 min incubation in a medium containing 0.20 M sucrose, WGA endosomal vesicles are not shown within the cytoplasm and green fluorescence is localized at the plasma membrane level (Fig. 5).

**Fig. 4a–c** Double labeling with WGA-FITC and dextran-TXR. Cells blocked in phagocytic activity are fed with WGA-FITC and dextran-TXR for 5 min (a, b), and fixed after a 20-min chase (c) in unlabeled medium. Both a and b are images of the same cell acquired at different focus planes. Bar: 20  $\mu$ m



As far as dextran is concerned, rare red vesicles are localized at a cortical level and in the cytoplasm. Thus, incubation of cells in hypertonic medium reduces uptake of both WGA and dextran, but the WGA uptake is reduced much more than that of the fluid phase marker.

Through cytosol acidification by 10 mM acetic acid, pH 5.0, WGA fluorescence is localized at the plasma membrane level, whereas small red vesicles containing dextran are localized both in the cortex, under the plasma membrane, and throughout the cytoplasm (Fig. 6). A similar fluorescent pattern was seen by using chlorpromazine (0.5  $\mu$ g/mL) (data not shown), a cationic amphiphilic drug which inhibits clathrin-dependent, receptor-mediated endocytosis by reducing the number of coated pit-associated receptors at the cell surface (Wang et al. 1993; Sofer and Futherman 1995).

We next used filipin (0.1  $\mu$ g/mL) and nystatin (2  $\mu$ g/mL) to further differentiate the pathway of internalization for WGA and dextran. Filipin and nystatin are effective inhibitors of dextran internalization when added to *Paramecium* cells either before, or simultaneously with, the fluid phase marker (Figs. 7, 8). Actually, sterol-binding agents such as filipin and nystatin disrupt caveolar structure and function (Schnitzer et al. 1994).

## Discussion

In *Paramecium* the fluorescence amount internalized by endocytosis is less than that internalized by phagocytosis, even if an increased endocytic rate is obtained when food vacuole formation is blocked. In effect, evidence was provided by electron microscopy studies that the number of endocytic vesicles increased when food vacuole formation was blocked by trifluoperazine, a calmodulin antagonist (Allen et al. 1992). In addition, by means of a quantitative analysis, it was shown more specifically that the HRP influx rate

increased twofold when phagocytosis was blocked by propranolol, a  $\beta$ -adrenergic antagonist (Wyroba 1991). A relation between phagocytosis and endocytosis was also found in rabbit alveolar macrophages, when cells which previously phagocytized latex particles showed a decreased rate of peroxidase accumulation (Buys and Kaplan 1987). In *Acanthamoeba castellani*, the increased rate of phagocytosis suppressed pinocytosis, but the combined values of the two uptake systems were essentially constant (Bower 1977). Wyroba (1991) suggests that in *Paramecium* the increased fluid phase uptake indicates that the two pathways, though independent, may be limited by a membrane pool and/or energy requirements. Indeed, forskolin and phorbol ester, powerful stimulants of *Paramecium* phagocytosis (Wyroba 1987, 1989), reduce the HRP uptake rate.

As for fluid uptake capacity, a low endocytic rate was also found in *P. aurelia* (Wyroba 1991): the HRP amount internalized in paramecia was much lower than in amoebae and mammalian cells. This result agrees with data from Kaneshiro et al. (1989) about the uptake of small organic molecules: the ingestion rate of these compounds was about six times lower in *Paramecium* than that measured in *Tetrahymena*.

Data obtained in the present pulse-chase study on *P. primaurelia* by using fluorescent markers such as WGA and dextran partly agree with those reported for *P. multimicronucleatum* (Allen et al. 1992) and *Tetrahymena pyriformis* (Nilsson and van Deurs 1983), obtained in transmission electron microscopy (EM) using HRP and cationized ferritin, respectively. Exogenous fluid and plasma membrane components are internalized by vesicles which are first localized in the cortical region of the cell and then migrate in the cytoplasm and fuse with other endosomal compartments, until their content is transferred to the food vacuoles (Fig. 9). In the end, denaturation and digestion of both endosome and food

**Fig. 5a–f** Effect of hypertonic medium on fluid phase and membrane-mediated transport. Cells blocked in phagocytic activity are incubated in 0.20 M sucrose, WGA-FITC and dextran-TXR for 5 (a, d), 10 (b, e) and 15 min (c, f). (a, d), (b, e) and (c, f) are images of the same cell acquired at different focus planes. Sucrose inhibits WGA internalization and reduces dextran internalization (d, e, f). Bar: 20  $\mu$ m

**Fig. 6a–c** Effect of cytosol acidification on fluid phase and membrane-mediated transport. Cells blocked in phagocytic activity are incubated in 10 mM acetic acid, pH 5.0, WGA-FITC and dextran-TXR for 5 min. Images are acquired at different focus planes from the ventral side (a) to the internal cytoplasm (b, c). Green fluorescence is localized on the plasma membrane and red fluorescence in vesicles in both the cortical region and throughout the cytoplasm. Bar: 20  $\mu$ m

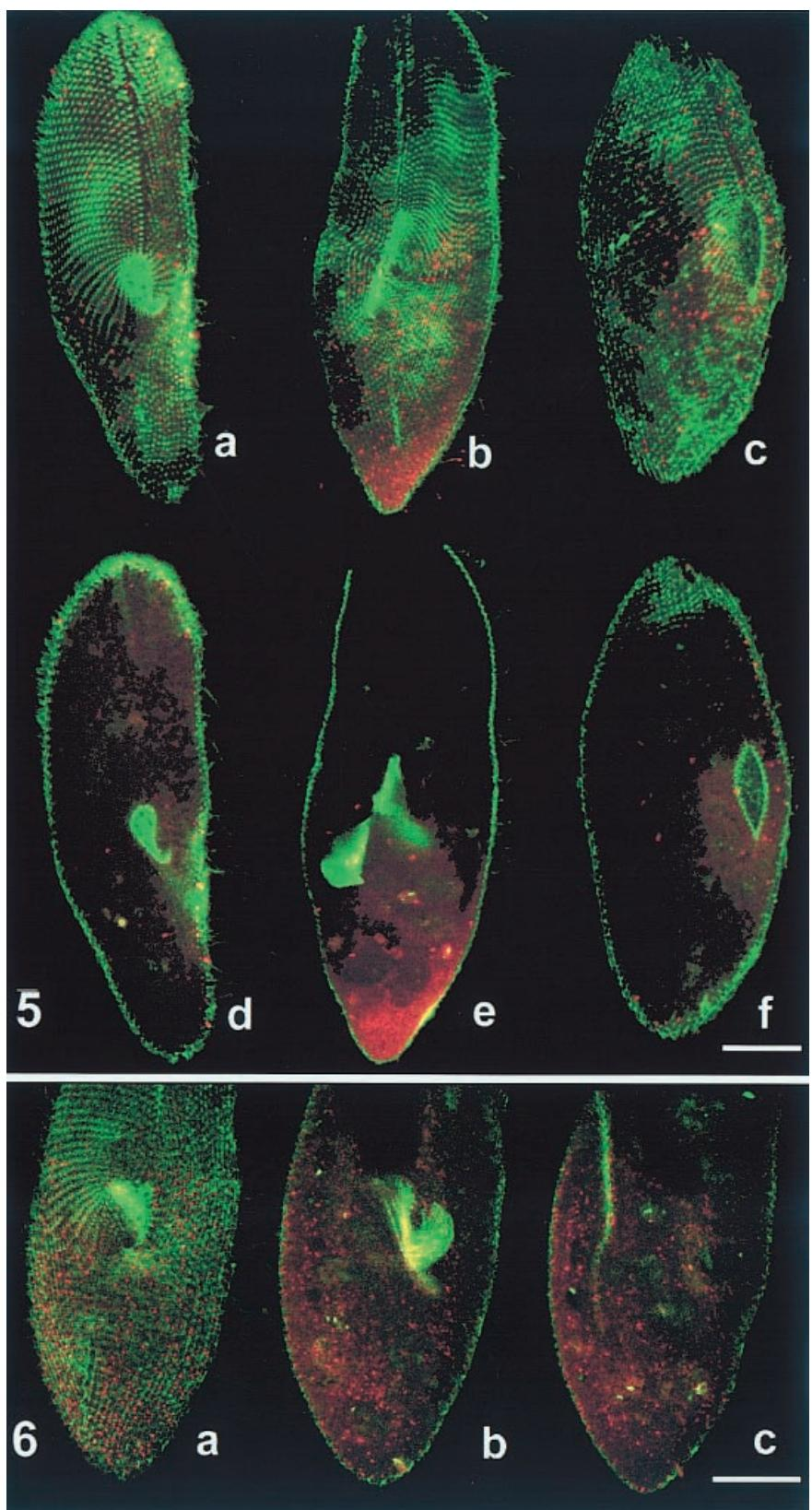
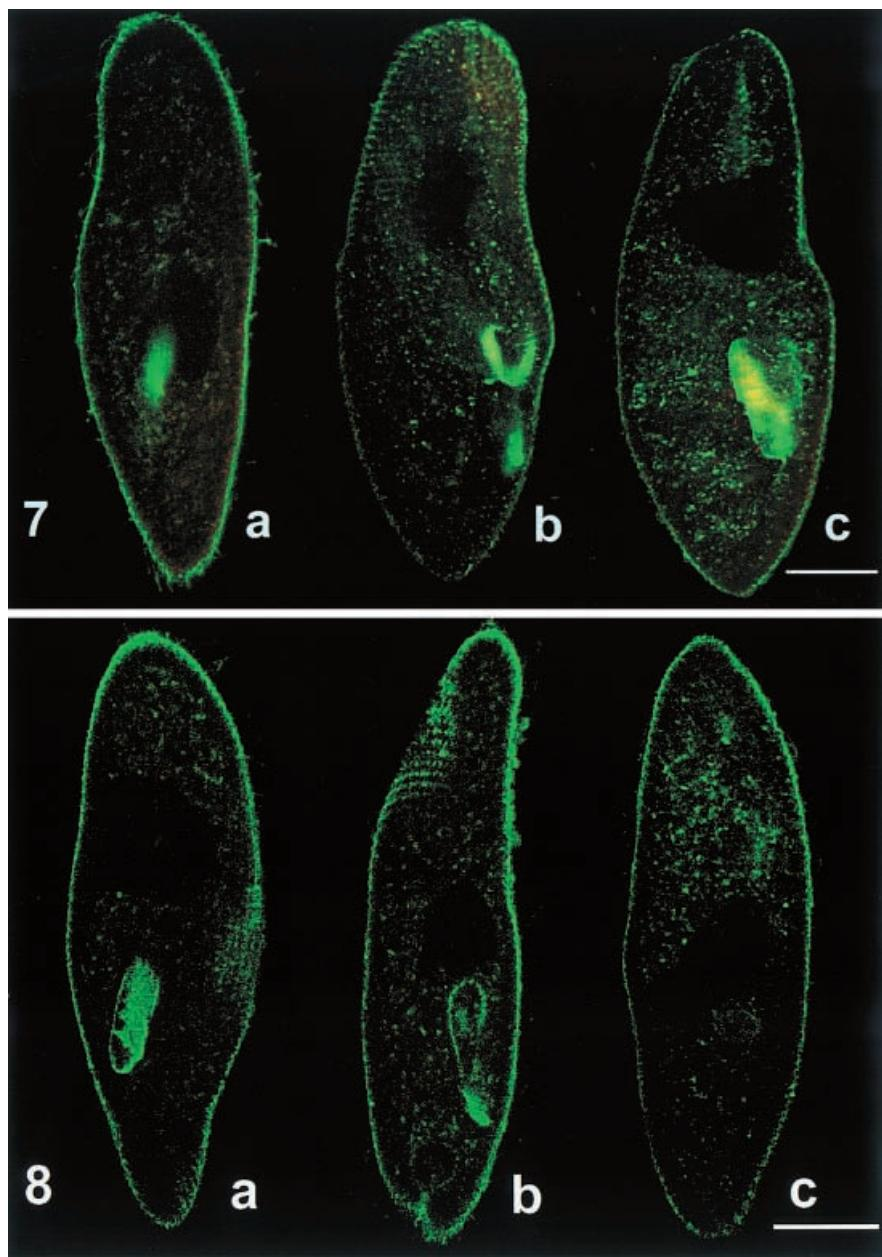


**Fig. 7a–c** Effect of nystatin on fluid phase and membrane-mediated transport. Cells blocked in phagocytic activity are incubated in 2 µg/mL nystatin, WGA-FITC and dextran-TXR for 5 (a), 10 (b) and 15 min (c). Green fluorescence is located on the plasma membrane and in vesicles through the cytoplasm; no red vesicles are seen inside the cell. Bar: 20 µm

**Fig. 8a–c** Effect of filipin on fluid phase and membrane-mediated transport. Cells blocked in phagocytic activity are incubated in 0.1 µg/mL filipin, WGA-FITC and dextran-TXR for 5 (a), 10 (b) and 15 min (c). Filipin inhibits red dextran fluorescence internalization. Bar: 20 µm



vacuole contents are completed together. The EM studies showed that HRP is internalized via coated pits and vesicles (Allen et al. 1992). Both coated pits and vesicles are labeled by the immunogold technique when a monoclonal antibody raised against the plasma membrane of *P. multimicronucleatum* (Allen et al. 1992) or a monoclonal antibody raised against the cell surface (glyco-)proteins (surface antigens) of *P. tetraurelia* (Flötenmeyer et al. 1999) is applied to sections of fixed cells. These data suggest that fluid phase marker internalization occurs at the clathrin-coated pits, as shown for receptor-mediated endocytosis. Conversely, we found by double-labeling experiments that, in *P. primaurelia*, WGA and dextran are taken up and transferred into the cell by two different vesicle popu-

lations, which then can fuse together or with food vacuoles. In order to understand if the two markers are internalized through two separate pathways, cells were incubated either in a hypertonic medium or in acetic acid. Indeed, subjecting mammalian cells to either incubation in media containing sucrose (Daukas and Zigmond 1985) or cytosol acidification with acetic acid (Davoust et al. 1987; Sandvig et al. 1987) has been shown to inhibit clathrin-mediated endocytosis by interfering with clathrin-adaptor interactions (Hansen et al. 1993b), or by altering the structure of clathrin itself (Heuser 1989; Heuser and Anderson 1989; Hansen et al. 1993a).

In *P. primaurelia*, 0.20 M sucrose incubation completely blocks the internalization of WGA, which stops

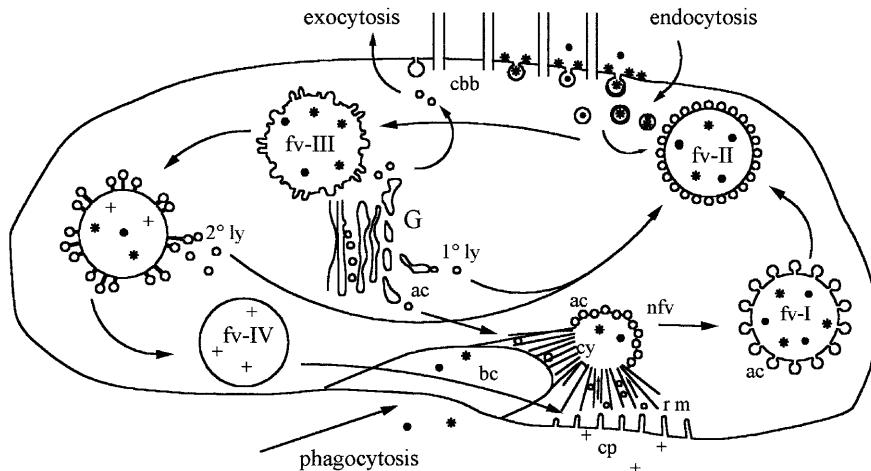


**Fig. 9** Schematic drawing of phagocytic and endocytic pathways of internalization in *Paramecium* based upon WGA-FITC and dextran-TXR staining. Without phagocytosis inhibition the ingested material is directed by the oral membranelle beating into the buccal cavity (*bc*), the cytopharynx (*cy*) and, finally, into the nascent food vacuole (*nfv*). The newly formed food vacuole (*fv-I*) is surrounded by acidosomes (*ac*) discharging their content into it. The vacuole reduces its size by eliminating water and membrane through small pinocytic vesicles. The condensed vacuole (*fv-II*) receives the enzymes contained into the primary (*1° ly*) and secondary lysosomes (*2° ly*). The cargo is digested (*fv-III*) and pinocytic vesicles containing digestion products are pinched off. Finally, the indigestible material (*fv-IV*) is excreted at the cytoproct (*cp*), while the vacuolar membrane is retrieved (*rm*). The endocytosis of WGA-FITC and dextran-TXR also occurs at the parasomal sacs located next to the ciliar basal bodies (*cbb*). Exogenous fluid and plasma membrane components are internalized by vesicles which fuse with food vacuoles, and the denaturation and digestion of endosome and food vacuole contents are completed together. *G* = Golgi apparatus; \* = WGA-FITC; ● = dextran-TXR; + = degraded material; → = flow direction (modified from Allen and Fok 2000)

at the plasma membrane. It also reduces dextran uptake, which is localized in small vesicles in the cortical part of the cell and in a few vesicles throughout the cytoplasm. A reduced uptake of probes in a hypertonic medium, but with the uptake of the receptor-mediated endocytosis probe reduced much more than that of the fluid phase marker, was also found in isolated rat hepatocytes (Synnes et al. 1999). However, conflicting results were obtained in mammalian cells as regards fluid phase endocytosis inhibition. In isolated rat hepatocytes, lucifer yellow endocytosis was not inhibited by sucrose (Oka and Weigel 1989; Oka et al. 1989), and in polymorphonuclear leukocytes, inhibition was independent from the solute used to increase tonicity (Daukas and Zigmund 1985). This is in contrast to HRP uptake experiments in 3T3 L1 fibroblasts (Carpentier et al. 1989) and in baby hamster kidney cells (Davoust et al. 1987), where the marker internalization was reduced after exposure to hypertonic medium.

In *Paramecium*, cytoplasm acidification and chlorpromazine block WGA uptake, not dextran internalization. Acidification of the cytosol of a number of different cell lines reduced the endocytotic uptake of

transferrin, even if the number of transferrin binding sites at the cell surface was increased (Sandvig and van Deurs 1996). In contrast, acidification has just a slight effect on the uptake of fluid phase marker lucifer yellow. Ricin is internalized by both clathrin-dependent and -independent endocytic mechanisms (Sandvig and van Deurs 1996, 1999) and a large portion of internalized toxin is transported to lysosomes for degradation. EGF, insulin and cytokine receptors, for instance, can also be endocytosed in the absence of functional clathrin-coated structures (Subtil et al. 1994).

Conversely, dextran internalization is blocked by filipin and nystatin, sterol-binding agents that disrupt caveolar structure and function (Schnitzer et al. 1994).

In conclusion, the data reported here indicate that WGA and dextran enter the cell via two distinct vesicle populations and that in *Paramecium*, as in mammalian cells, fluid phase endocytosis is unaffected by treatments that arrest coated pit-mediated endocytosis, indicating that fluid phase endocytosis is primarily clathrin independent.

**Acknowledgements** This work was supported by grants from Genoa University and INFM (Italy).

## References

- Allen RD (1988) Cytology. In: Götz H-D (ed) *Paramecium*. Springer, Berlin Heidelberg New York, pp 4–40
- Allen RD, Fok AK (1993) Endosomal membrane traffic of ciliates. In: Plattner H (ed) Advances in cell and molecular biology of membranes. Membrane traffic in protozoa. JAI Press, Greenwich, Conn., pp 283–309
- Allen RD, Fok AK (2000) Membrane trafficking and processing in *Paramecium*. *Int Rev Cytol* 198:277–318
- Allen RD, Ueno MS, Fok AK (1988) A survey of lectin binding in *Paramecium*. *J Protozool* 35:400–407
- Allen RD, Schroeder CC, Fok AK (1992) Endosomal system of *Paramecium*: coated pits to early endosomes. *J Cell Sci* 101:449–461
- Bower B (1977) Comparison of pinocytosis and phagocytosis in *Acanthamoeba castellanii*. *Exp Cell Res* 110:409–427
- Buyss SS, Kaplan J (1987) Effect of phagocytosis on receptor distribution and endocytic activity in macrophages. *J Cell Physiol* 131:442–449

- Carpentier JL, Sawano F, Geiger D, Gorden P, Perrelet A, Orci L (1989) Potassium depletion and hypertonic medium reduce "non-coated" and clathrin-coated pit formation, as well as endocytosis through these gates. *J Cell Physiol* 138:519–526
- Chapman-Andresen C (1962) Studies on pinocytosis in *Amoebae*. C R Trav Lab Carlsberg 33:73–264
- Courtois PJ (1989) Dissection of endosomes. In: Steer C, Hanover J (eds) Intracellular trafficking of proteins. Cambridge University Press, New York, pp 103–156
- Daukas G, Zigmund SH (1985) Inhibition of receptor-mediated but not fluid-phase endocytosis in polymorphonuclear leukocytes. *J Cell Biol* 101:1673–1679
- Davoust J, Gruenberg J, Howell KE (1987) Two threshold values of low pH block endocytosis at different stages. *EMBO J* 6:3601–3609
- Deurs B van, Petersen OW, Olsnes S, Sandvig K (1989) The ways of endocytosis. *Int Rev Cytol* 117:131–177
- Diaspro A, Beltrame F, Fato M, Ramoino P (1996) Wide-field and confocal optical sectioning microscopy for 2-D/3-D characterization of biostructure and of cellular events. *IEEE Eng Med Biol* 15:92–100
- Diaspro A, Annunziata S, Raimondo M, Ramoino P, Robello M (1999) A single pinhole confocal laser scanning microscope for 3-D imaging of biostructure. *IEEE Eng Med Biol* 18:106–110
- Flötenmeyer M, Momayez M, Plattner H (1999) Immunolabeling analysis of biosynthetic and degradative pathways of cell surface components (glycocalyx) in *Paramecium* cells. *Eur J Cell Biol* 78:67–77
- Gruenberg J, Howell KE (1989) Membrane traffic in endocytosis: insights from cell-free assay. *Annu Rev Cell Biol* 5:453–481
- Hansen SH, Sandvig K, Deurs B van (1993a) Clathrin and HA2 adaptors: effects of potassium depletion, hypertonic medium, and cytosol acidification. *J Cell Biol* 121:61–72
- Hansen SH, Sandvig K, Deurs B van (1993b) Molecules internalized by clathrin-independent endocytosis are delivered to endosomes containing transferrin receptors. *J Cell Biol* 123:89–97
- Heuser J (1989) Effects of cytoplasmic acidification on clathrin lattice morphology. *J Cell Biol* 108:401–411
- Heuser JE, Anderson RG (1989) Hypertonic media inhibit receptor-mediated endocytosis by blocking clathrin-coated pit formation. *J Cell Biol* 108:389–400
- Kaneshiro ES, Merkel SJ, Reuter SF (1989) Uptake and utilization of small molecules by *Paramecium tetraurelia*. *Eur J Cell Biol* 49:55–60
- Lamaze C, Schmid SL (1995) The emergence of clathrin-independent pinocytic pathways. *Curr Opin Cell Biol* 7:573–580.
- Mellman I, Howe C, Helenius A (1987) The control of membrane traffic on the endocytic pathway. *Curr Top Membr Transp* 29:255–288
- Nilsson JR, Deurs B van (1983) Coated pits and pinocytosis in *Tetrahymena*. *J Cell Sci* 63:209–222
- Oka JA, Weigel PH (1989) The pathways for fluid phase and receptor mediated endocytosis in rat hepatocytes are different but thermodynamically equivalent. *Biochem Biophys Res Commun* 159:488–494
- Oka JA, Christensen MD, Weigel PH (1989) Hyperosmolarity inhibits galactosyl receptor-mediated but not fluid phase endocytosis in isolated rat hepatocytes. *J Biol Chem* 264:12016–12024
- Ramoino P (1997) Lectin-binding glycoconjugates in *Paramecium primaurelia*: changes with cellular age and starvation. *Histochemistry Cell Biol* 107:321–329
- Ramoino P, Beltrame F, Diaspro A, Fato M (1996) Time-variant analysis of organelle and vesicle movement during phagocytosis in *Paramecium primaurelia* by means of fluorescence confocal laser scanning microscopy. *Microsc Res Tech* 35:377–384
- Sandvig K, Deurs B van (1996) Endocytosis, intracellular transport, and cytotoxic action of Shiga toxin and ricin. *Physiol Rev* 76:949–966
- Sandvig K, Deurs B van (1999) Endocytosis and intracellular transport of ricin: recent discoveries. *FEBS Lett* 452:67–70
- Sandvig K, Olsnes S, Petersen OW, Deurs B van (1987) Acidification of the cytosol inhibits endocytosis from coated pits. *J Cell Biol* 105:679–689
- Schnitzer JE, Oh P, Pinney E, Allard J (1994) Filipin-sensitive caveolae-mediated transport in endothelium: reduced transcytosis, scavenger endocytosis, and capillary permeability of selected macromolecules. *J Cell Biol* 127:1217–1232
- Sofer A, Futherman AH (1995) Cationic amphiphilic drugs inhibit the internalization of cholera toxin to the Golgi apparatus and the subsequent elevation of cyclic AMP. *J Biol Chem* 270:12117–12122
- Stockem W (1977) Endocytosis. In: Jamieson GA, Robinson DM (eds) Mammalian cell membranes, vol 5. Butterworths, London, pp 151–195
- Stockem W, Wohlfarth-Bottermann KE (1969) Pinocytosis (endocytosis). In: Lima de Faria A (ed) Handbook of molecular cytology, North Holland, Amsterdam, pp 1373–1400
- Subtil A, Hemar A, Dautry-Varsat A (1994) Rapid endocytosis of interleukin 2 receptors when clathrin-coated pit endocytosis is inhibited. *J Cell Sci* 107:3461–3468
- Synnes M, Prydz K, Lovdal T, Brech A, Berg T (1999) Fluid phase endocytosis and galactosyl receptor-mediated endocytosis employ different early endosomes. *Biochim Biophys Acta* 1421:317–328
- Wang L-H, Rothberg KG, Anderson RGW (1993) Mis-assembly of clathrin lattices on endosomes reveals regulatory switch for coated pit formation. *J Cell Biol* 123:1107–1117
- Wyroba E (1987) Stimulation of *Paramecium* phagocytosis by phorbol ester and forskolin. *Cell Biol Int Rep* 11:657–664
- Wyroba E (1989) Beta-adrenergic stimulation of phagocytosis in the unicellular eukaryote *Paramecium aurelia*. *Cell Biol Int Rep* 13:667–678
- Wyroba E (1991) Quantitation of fluid phase uptake in *Paramecium*. 1. Kinetics in the cells blocked in phagocytic activity. *Cell Biol Int Rep* 15:1207–1216